DOI: 10.21776/ub.jpacr.2025.015.01.8000 *J. Pure App. Chem. Res.*, **2026**, 15 (1), 12-25
5 April 2026

# Molecular Dynamics Simulation of Heparin 8 and 12 Saccharides With 2S Sulfation Pattern and 1C4 Iduronate Conformation To FGF2-FGFR1 Ternary Complex As Environmentally Friendly Anticancer Drug Candidate Discovery

Himmatul Barroroh[1,2,*], Muhammad Mazyadi[1], Lukman Hakim[2], Anna Safitri[2], and Widodo Widodo[3]

[1]Chemistry Department, Universitas Islam Negeri Maulana Malik Ibrahim Malang, Jl. Gajayana No.50 Malang, East Java, Indonesia, 65144
[2]Chemistry Department, Faculty of Mathematics and Natural Sciences, Brawijaya University, Jl. Veteran Malang, East Java, Indonesia, 65145
[3]Biology Department, Faculty of Mathematics and Natural Sciences, Brawijaya University, Jl. Veteran Malang, East Java, Indonesia, 65145

[*] Corresponding Author: himmatul.b@kim.uin-malang.ac.id, ORCHID ID: 57209801096

Received 25 November 2025; Accepted 17 February 2026

## ABSTRACT

Heparin is a linear polysaccharide composed of repeating 1–4 linked units of iduronic acid and glucosamine and is widely used as an anticoagulant drug. This paper reports characteristics of three-dimensional structural changes and stability of the FGF2–FGFR1 ternary complex in the presence of heparin 8- and 12-saccharide fragments with a 2S sulfation pattern and ^1C$_4$ iduronate conformation using in silico approach. Study was performed using molecular docking followed by 100 ns molecular dynamics (MD) simulations. Heparin 8- and 12-saccharide ligands were docked to the FGF2–FGFR1 ternary complex, then was evaluated by MD using GROMACS to monitor backbone root mean square deviation (RMSD), residue root means square fluctuation (RMSF), and key residue interactions over time. Docking suggested a more favorable initial binding energy for the 8-saccharide ligand, whereas MD revealed that the 12-saccharide ligand more effectively maintained stable interactions between FGF2 and FGFR1, as indicated by lower backbone RMSD at the end of the simulation and more persistent contacts at basic residues in the heparin-binding sites of both proteins. These dynamic stability features provide a mechanistic explanation for previously reported in vitro findings, showing that 12-saccharide 2S heparin fragments exert stronger FGF2-dependent antiangiogenic and anticancer effects than shorter fragments, thereby supporting their potential as environmentally friendly anticancer drug candidates.

Keywords: Heparin; FGF2–FGFR1 ternary complex; molecular docking; molecular dynamics simulation; anticancer drug candidate

## INTRODUCTION

Cancer is the second leading cause of death in the world after cardiovascular disease and is projected to become the leading cause of death in the next few years. Global Cancer Observatory data in 2022 shows that the incidence of cancer reached 18,741,966 cancer cases around the world [1]. Cancer is one of the most significant public health challenges of the 21st century. The large data on cancer deaths of 9.7 million globally has encouraged research and development of drugs that are able to overcome this problem [2].

The journal homepage www.jpacr.ub.ac.id
p-ISSN : 2302 – 4690 | e-ISSN : 2541 – 0733

Despite substantial advances in cancer treatment, conventional therapeutic approaches such as chemotherapy, radiotherapy, and targeted therapy remain limited by severe side effects, high treatment costs, and the emergence of drug resistance. Chemoresistance and systemic toxicity frequently compromise therapeutic efficacy, while targeted therapies often fail to achieve sustained clinical responses due to pathway redundancy and adaptive resistance mechanisms [3, 4]. Therefore, it is urgent to develop alternative or complementary therapeutic agents that modulate key signaling pathways involved in tumour growth and angiogenesis.

Heparin is widely known as a polysaccharide that functions as an anticoagulant drug [5]. Heparin is a linear polysaccharide characterized by repeating disaccharide units of glucosamine (GlcN) and uronic acids, predominantly iduronic acid (IdoA). The use of heparin in cancer treatment has long been investigated due to its ability to attenuate tumor growth, angiogenesis, and metastasis [5-9]. However, the molecular mechanisms underlying the dependence of heparin's anticancer activity on oligosaccharide length, sulfation pattern, and iduronate conformation remain incompletely understood.

During biosynthesis, the heparin chain undergoes extensive modifications, including N-sulfation and O-sulfation, particularly 2-O-sulfation (2S) of iduronic acid residues, which strongly influence its biological activity. The biological function of heparin is closely associated with its structure–function relationship. The 2-O-sulfated iduronic acid (IDS) residue has three possible conformations, namely $^4C_1$, $^1C_4$, and $^2S_0$. Previous studies have demonstrated that specific iduronate conformations and sulfation patterns modulate the affinity of heparin toward fibroblast growth factors (FGFs) and their receptors. The $^2S_0$ conformation of iduronate has been reported to exhibit high-energy interactions with N-sulfated glucosamine in FGF binding, whereas the $^4C_1$ and $^1C_4$ conformations tend to support more transient interactions [10-11]. At the molecular level, sulfation pattern and iduronate conformation govern electrostatic interactions and hydrogen bonding between negatively charged sulfate groups and basic amino acid residues on the protein surface. These interactions play a critical role in stabilizing protein–ligand complexes and regulating downstream signaling pathways associated with angiogenesis and cancer progression. Among the FGF family, fibroblast growth factor 2 (FGF2) and fibroblast growth factor receptor 1 (FGFR1) play a pivotal role in cancer development by regulating angiogenesis, cell proliferation, survival, and migration. Aberrant activation of the FGF2–FGFR1 signaling pathway has been implicated in enhanced tumor vascularization and metastatic potential in various cancers [10]. Heparin functions as a co-factor in this pathway by stabilizing the FGF2-FGFR1 ternary complex, facilitating receptor dimerization and signal transduction; therefore, modulation of this interaction is highly relevant for anticancer therapy [12]. Although molecular docking studies of the FGF2-FGFR1-heparin complex have been previously reported, comparative molecular dynamics investigations focusing on specific heparin chain lengths and conformational features are still limited. In particular, no study has systematically compared long-timescale (100 ns) molecular dynamics simulations of 8- and 12-saccharide heparin fragments with a 2-O-sulfation pattern and $^1C_4$ iduronate conformation to explain differences observed in in vitro anticancer activity.

Therefore, this study aims to investigate the structural stability and dynamic behavior of the FGF2–FGFR1 ternary complex in the presence of heparin 8- and 12-saccharide fragments with a 2-O-sulfation pattern and $^1C_4$ iduronate conformation by an in silico approach. By integrating molecular docking with 100 ns molecular dynamics simulations, this work bridges static binding predictions with dynamic stability analysis and correlates the computational findings with previously reported in vitro data by Cole et al. [13], therefore can provide a



The journal homepage www.jpacr.ub.ac.id
p-ISSN : 2302 – 4690 | e-ISSN : 2541 – 0733

mechanistic explanation for the length-dependent anticancer and antiangiogenic effects of heparin oligosaccharides.

## METHOD

### Crystal structure data

Crystal structure used in this research are the three-dimensional structures of the FGF2–FGFR1 ternary complex receptor with PDB ID code 1FQ9 and the heparin 8- and 12-saccharide ligands with 2S sulfation pattern and iduronate ^1C$_4$ conformation derived from PDB ID code 1HPN.

### Computational environment

All computational analyses were performed on a workstation equipped with a multi-core Intel® processor, 32 GB RAM, and a Linux-based operating system. Molecular docking was conducted using AutoDock 4.2, while AutoDockTools was used for ligand and receptor preparation. Structural visualization and inspection were carried out using UCSF Chimera and PyMOL. Molecular dynamics simulations were performed using GROMACS, and glycan preparation and parameterization were conducted via CHARMM-GUI employing the CHARMM36 force field. Discovery Studio Visualizer (2021) was used as the primary platform for interaction analysis and visualization.

### Preparation of FGF2–FGFR1 ternary complex as macromolecules

Protein structure was downloaded from the RCSB Protein Data Bank (https://www.rcsb.org) with PDB code 1FQ9. Preparation was carried out using UCSF Chimera. Ligand and receptor were separated, missing atoms and residues were modeled using MODELLER, hydrogen atoms were added, and charges were assigned for standard residues using the AMBER ff14SB method and for other residues using the AM1-BCC method. Although the crystal structure of 1FQ9 has a resolution of 3.0 Å, it was selected because it represents a well-characterized FGF2–FGFR1–heparin ternary complex that explicitly contains the heparin-binding site and key residues required for mechanistic evaluation.

### Heparin ligand preparation

Ligand used was a heparin molecule downloaded from the RCSB Protein Data Bank with PDB code 1HPN. Visualization was performed using PyMOL, and the structure with iduronate ^1C$_4$ conformation was selected. The $SO_3$ group attached to the SGN residue was removed and replaced with a hydrogen atom to generate a 2-O-sulfated iduronate (2S) structure. Heparin oligosaccharides with lengths of 8 and 12 saccharides were constructed accordingly.

The prepared heparin ligands were further processed using AutoDockTools by adding Gasteiger charges and assigning AD4 atom types. Free torsions were defined on the heparin backbone with a maximum of 32 rotatable bonds.

### Validation of molecular docking procedure

Validation of the docking protocol was performed by redocking the native heparin ligand into the FGF2-FGFR1 ternary complex using AutoDock 4.2 [14]. The Lamarckian Genetic Algorithm (LGA) was applied with 200 GA runs. The grid box was centered on the native ligand position, with dimensions set to twice the longest axis of the ligand. A rigid docking approach was employed primarily to validate the native binding pose and to enable an initial comparison of binding energies. Given the high intrinsic flexibility of heparin, conformational adaptability was subsequently addressed during molecular dynamics simulations. The use of a



The journal homepage www.jpacr.ub.ac.id
p-ISSN : 2302 – 4690 | e-ISSN : 2541 – 0733

rigid receptor with a flexible ligand is therefore considered appropriate for initial screening prior to long-timescale MD simulations.

**Molecular docking of test heparin ligands**

Molecular docking was conducted for heparin 8-2S-1$C_4$ and 12-2S-1$C_4$ ligands against the FGF2–FGFR1 ternary complex using AutoDockTools. The grid box parameters were adjusted according to ligand size, with a grid spacing of 0.375 Å. Docking results were evaluated based on binding energy and interaction patterns.

**Analysis of docking results**

Visualization of docking interactions was performed using AutoDockTools and Discovery Studio Visualizer [15]. AutoDockTools was mainly used to inspect ligand poses and binding energies, whereas Discovery Studio Visualizer served as the primary platform for identifying hydrogen bonds, electrostatic interactions, and key residue contacts.

**Molecular dynamics simulation preparation**

Preparation of the docked complexes for molecular dynamics simulations was carried out using the Glycan Reader & Modeler module available on the CHARMM-GUI platform. The CHARMM36 force field, which includes parameters for carbohydrates and glycans, was applied. The system was solvated using the TIP3P water model in a cubic simulation box with a 15 Å buffer distance. $Na^+$ and $Cl^-$ ions were added to neutralize the system and mimic physiological ionic conditions.

**Molecular dynamics simulation**

Molecular dynamics simulations were performed using GROMACS [16]. Energy minimization was conducted to remove unfavorable contacts, followed by equilibration under NVT conditions at 310 K for 2 ns and subsequent NPT equilibration at 1 atm. The production phase was carried out for 100 ns with a time step of 1 fs. Trajectory data were analyzed to determine backbone RMSD, residue RMSF, and ligand–protein interactions over the simulation period.

## RESULT AND DISCUSSION

**Preparation of FGF2-FGFR1 ternary complex macromolecule**

FGF2-FGFR1 ternary complex macromolecule obtained from the RCSB Protein Data Bank with code 1FQ9 (Figure 1) is a structure containing two dimeric proteins and two bound ligands as a result of X-ray diffraction. The two dimer proteins are FGF2 which consists of chains A and B and FGFR1 which consists of chains C and D, while the two native ligands are heparin with an oligomer length of 8 saccharides and 6 saccharides with a 2SNS6S sulfation pattern. The FGF2-FGFR1 ternary complex macromolecule is separated from the two native ligands and then used as a macromolecular entity to which the test ligand will be attached. The separation process was carried out in the UCSF Chimera software by removing all non-standard residues namely IDS, SGN, IDU, and UAP.



The journal homepage www.jpacr.ub.ac.id
p-ISSN : 2302 – 4690 | e-ISSN : 2541 – 0733

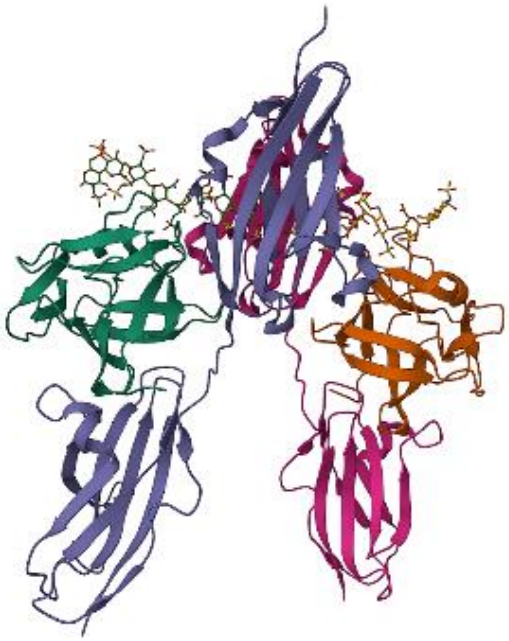

**Figure 1.** Structure of the FGF2-FGFR1-Heparin complex, FGF2 A chain (green ribbon), FGF2 B chain (orange ribbon), FGFR1 C chain (violet ribbon), FGFR1 D chain (red ribbon). Heparin native ligand 8 saccharides (ball and stick-left), heparin native ligand 6 saccharides (ball and stick - right).

**Heparin ligand preparation**

Heparin test ligand was obtained from the RCSB Protein Data Bank with code 1HPN (Figure 2). The structure of 1HPN consists of 2 sulfated heparin 12 saccharide molecule with sulfation pattern of 2SNS6S with two conformations of iduronic acid, namely $^{2}S_{0}$ and $^{1}C_{4}$ respectively. This structure contains a repeating chain of glucosamine (SGN) and iduronic acid

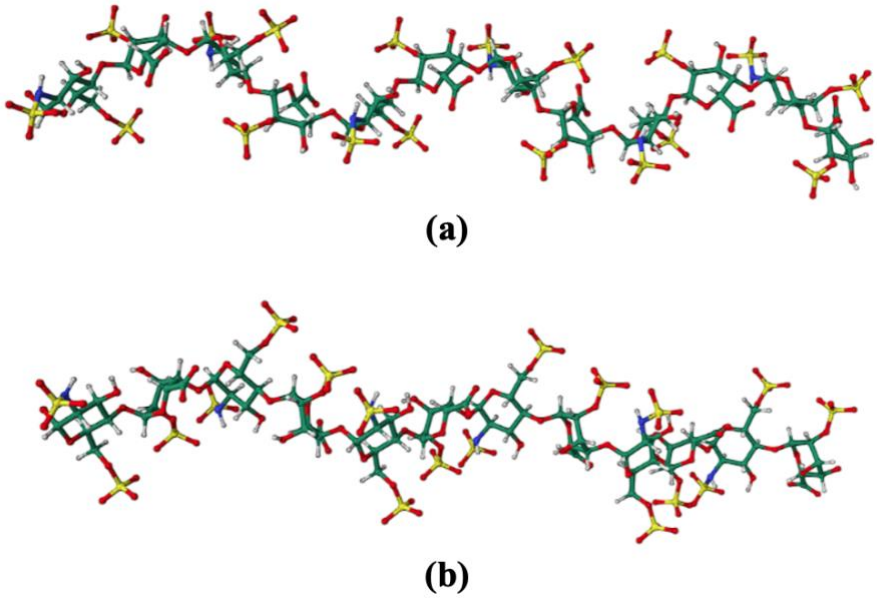


**Figure 2.** (a) Heparin (1HPN) $^{2}S_{0}$ conformation (b) Heparin (1HPN) $^{1}C_{4}$ conformation



The journal homepage www.jpacr.ub.ac.id
p-ISSN : 2302 – 4690 | e-ISSN : 2541 – 0733

(IDS) residues in the order SGN1-IDS2-SGN3-IDS4-SGN5-IDS6-SGN7-IDS8-SGN9-IDS10 -SGN11-IDS12. $SO_3$ group attached to the SGN residue is cut to form sulfated heparin Iduronate 2-O-Sulfate (2S) and an H atom is added to repair the bond that has been cut (Figure 3). The cut heparin ligand was prepared using AutodockTool software, with a Gasteiger charge added and AD4 Type atomic assignments. The hydrogen atoms are arranged according to non-polar mergers so that only polar hydrogen will interact with the protein [17].

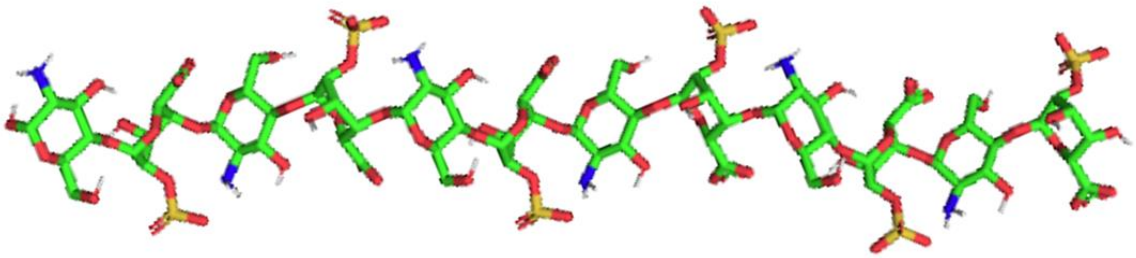

**Figure 3.** Test ligand of 2S sulfated heparin 12 saccharide with IDS $^1C_4$ conformation

**Validation of native ligand redocking**

Results of redocking native heparin ligand with 8 saccharides to the FGFR1-FGF2 ternary complex using Autodock were able to place the native ligand back into the initial heparin binding site with an RMSD value of 1.06 Å and a binding energy value of -34.22 kcal/mol (Tabel 1.).

**Table 1.** Redocking parameter of 1FQ9 native ligand

| PDB Code | Grid Center | | | RMSD (Å) | Binding Energy (kcal/mol) |
|---|---|---|---|---|---|
| | *X* | *Y* | *Z* | | |
| 1FQ9 | 80.459 | 23.095 | 104.054 | 1.06 | -34.22 |

Redocking of molecules also indicates interactions between ligand and receptor at residues (Table 2). The results of redocking the native ligand with the FGFR1-FGF2 protein can be seen in Figure 4. Redocking native ligand in the FGFR1-FGF2 receptor has residue interactions that are similar to those of the native ligand.

**Table 2.** Interaction of native docking and redocking results

| Ligand | Interaction of Docking Results |
|---|---|
| Native | Ala 136, Arg 120, Asn 27, Lys 119, Lys 125, Lys 129, Lys 135, Lys 26, His 166, Lys 160, Lys 163, Lys 172, Lys 175, Lys 177, Lys 207, Thr 173 |
| Redocking native | Ala 136, Arg 120, Asn 27, Gln 134, Lys 119, Lys 125, Lys 129, Lys 135, Lys 26, His 166, Lys 160, Lys 163, Lys 172, Lys 175, Lys 177, Val 174, Lys 207 |



The journal homepage www.jpacr.ub.ac.id
p-ISSN : 2302 – 4690 | e-ISSN : 2541 – 0733

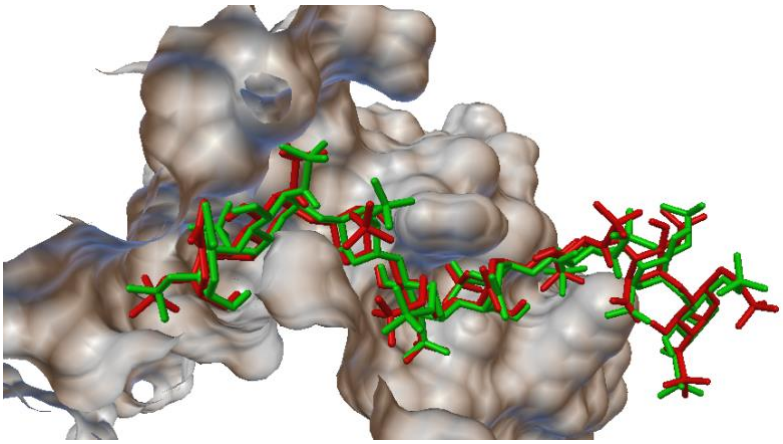

**Figure 4.** Overlay pose between the native heparin 8 saccharide ligand 1FQ9 (green) and the redocking result (red) in the heparin binding site region in the FGF2-FGFR1 ternary complex.

The redocking results also produced interactions on key amino acid residues, namely Ala 136, Arg 120, Asn 27, Lys 125, Lys 129, Lys 134, Lys 135, 160, Lys 163, Lys 172, and Lys 177. This shows the results of the docking validation of native ligand is valid, because it has an RMSD value ≤ 2.0 Å and interaction amino acid residues similar to native ligand interactions [18].

**Analysis of docking results**

Docking results of the heparin test ligand 8-2S-1C4 showed a binding energy that was smaller than that of the heparin test ligand 12-2S-1C4 (Table 3). The more negative the binding energy value produced, the better the level of stability of the bond between the ligand and receptor. The difference in binding energy values (negative/positive and small/high) for each compound is influenced by its molecular structure (the ligand 8-2S-1C4 is different from the ligand 12-2S-1C4). The lower the binding energy value, the more stable the protein and ligand bonds will be due to the greater the attractive forces between molecules and the repulsive forces becoming minimum so that the conformation is more stablee [19, 20].

**Table 3.** Docking test ligand parameter

| Ligand | Grid Center | | | Binding Energy (kcal/mol) |
|---|---|---|---|---|
| | *X* | *Y* | *Z* | |
| Heparin 8-2S-$^1C_4$ | 88.459 | 27.095 | 111.053 | -7.25 |
| Heparin 12-2S-$^1C_4$ | 82.540 | 26.378 | 111.967 | + 0.89 |



The journal homepage www.jpacr.ub.ac.id
p-ISSN : 2302 – 4690 | e-ISSN : 2541 – 0733

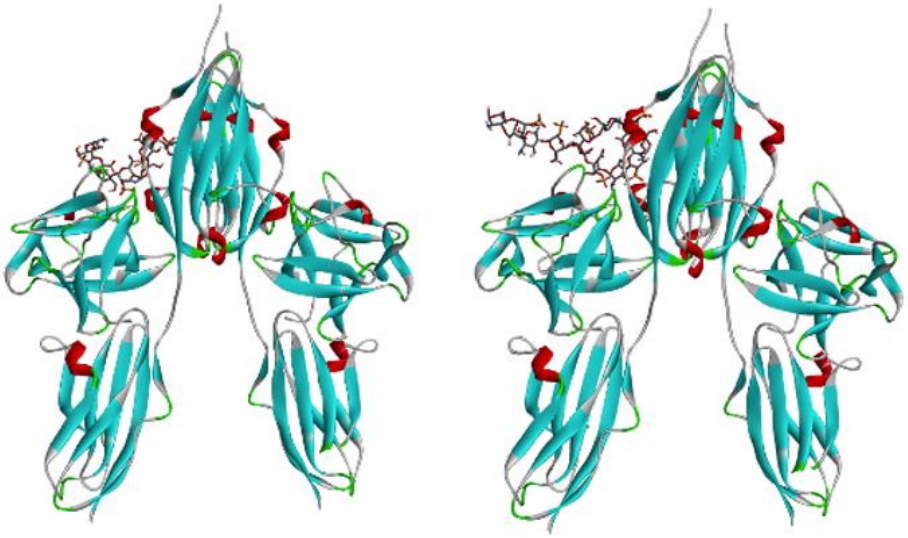

(a) Heparin 8-2S-$^{1}C_4$ (b) Heparin 12-2S-$^{1}C_4$

**Figure 5.** Results of ligand docking test for heparin 8-2S-$^{1}C_4$ and 12-2S-$^{1}C_4$.

On the docking, amino acid residues of the heparin ligand 8-2S-1C4 have interactions with more key residues than the heparin ligand 12-2S-1C4 (Tabel 4). This is possible because the heparin ligand 12-2S-1C4 molecule has a structure whose length exceeds the spatial dimensions of the binding site (Figure 5.). The outer end of the heparin test ligand 12-2S-1C4 appears to hang outside the binding site area thereby destabilizing the FGF2-FGFR1 ternary complex-ligand interaction. However, both have several key ligand interactions that are similar to native heparin, so it is still possible that they have the same biological function.

**Table 4.** Ligand-amino acid residue interaction of ternary FGF2-FGFR1 complex

| Heparin Ligand | Amino acid residue interaction of docking result | |
|---|---|---|
| | **Key Residue** | **Other Residue** |
| Native | Ala 136, Arg 120, Asn 27, Lys 125, Lys 129, Lys 135, Lys 160, Lys 163, Lys 172, Lys 177. | Lys 119, Lys 26, His 166, Lys 175, Lys 207, Thr 173. |
| 8-2S-$^{1}C_4$ | Arg 120, Asn 27, Gln 134, Lys 125, Lys 129, Lys 135, Lys 163, Lys 177. | Arg 209, Lys 207. |
| 12-2S-$^{1}C_4$ | Arg 120, Lys 125, Lys 129, Lys 135. | Lys 119, Glu 159, Arg 209. |

**Preparation of molecular dynamics simulation**

Preparation of the structural adaptation of the complex FGF2-FGFR1-heparin molecule from docking for use in molecular dynamics simulations was carried out using CHARMM-GUI with the Glycan Reader & Modeler module (Figure 6). This was necessary because glycan residues in the ligand are non-standard residues that cannot be automatically recognized in the Gromacs program.



The journal homepage www.jpacr.ub.ac.id
p-ISSN : 2302 – 4690 | e-ISSN : 2541 – 0733

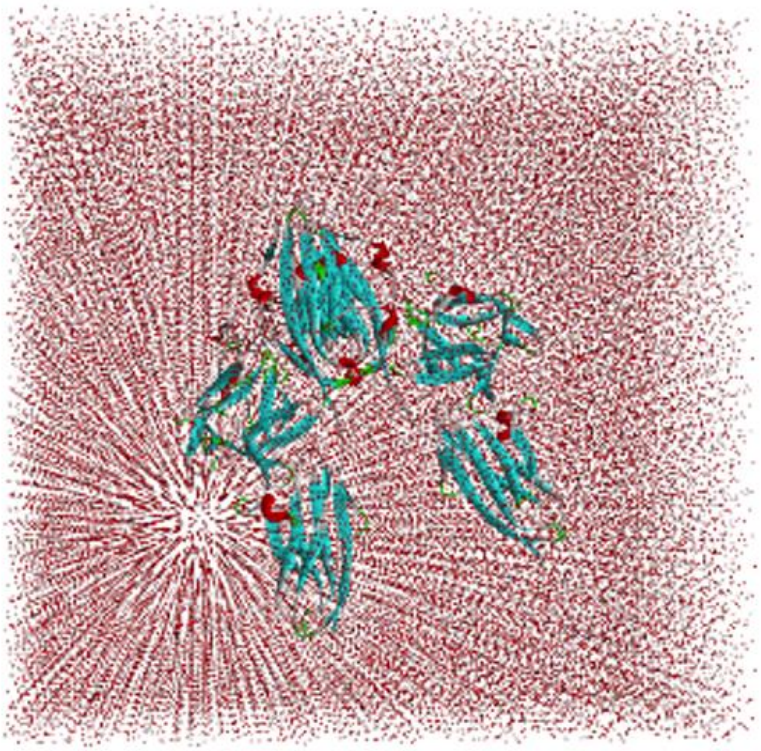

**Figure 6.** Simulation box of the FGF2-FGFR1-heparin complex in the form of a cube prepared using CHARMM-GUI.

**Molecular dynamics simulation**

Molecular dynamics simulations were carried out with production for 100 ns. The results obtained after going through the production stage of the molecular dynamics simulation are trajectory files containing the displacement of atomic positions and energy during the simulation. These results are then processed to obtain RMSD values for the protein backbone, RMSF of amino acid residues, and interactions between the ligand and the receptor.

**Root mean square deviation (RMSD) results of backbone protein, ligand and IDS conformation**

In a simulation that lasted for 100 ns, all three systems experienced an increase in protein backbone RMSD (Figure 7a-c). The backbone RMSD graph of the FGF2-FGFR1 ternary complex - native heparin 1FQ9 and the FGF2-FGFR1 ternary complex-heparin 8-2S-$^{1}C_{4}$ shows stability in the first 6 ns then increases, this shows stability in the early stages, then in the first 10 ns structures changes occur indicating conformational adjustments. Meanwhile, the FGF2-FGFR1 ternary complex-heparin 12-2S-$^{1}C_{4}$ showed an increase in RMSD values from the beginning indicating high conformational flexibility of the protein and then reached better stability at 45 ns [21].



The journal homepage www.jpacr.ub.ac.id
p-ISSN : 2302 – 4690 | e-ISSN : 2541 – 0733

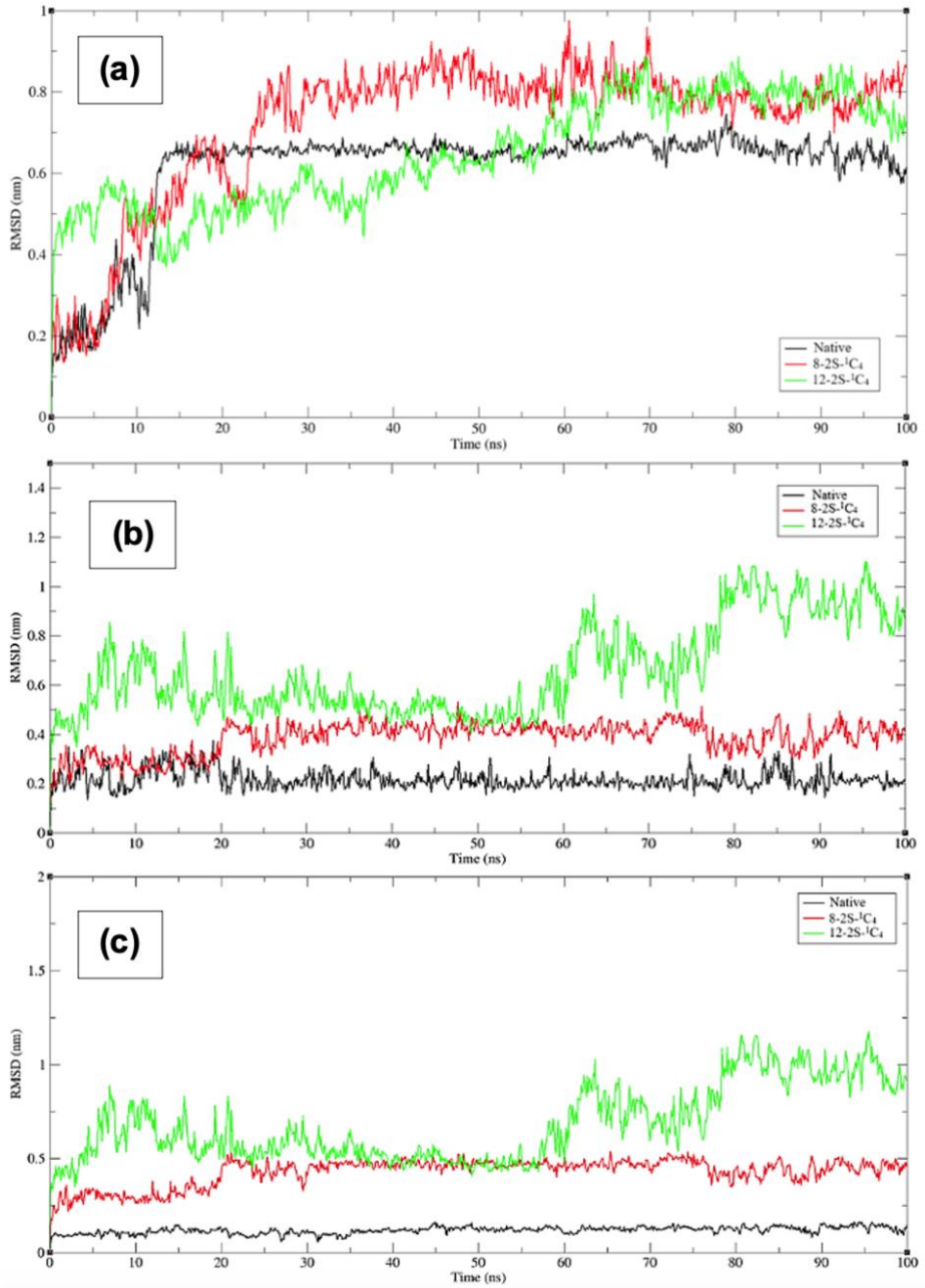


**Figure 7.** Graph of fluctuations in the backbone RMSD values for: **(a)** the FGF2-FGFR1-heparin ternary complex protein during a simulation time of 100 ns. (Black line is native, FGF2-FGFR1-heparin ternary complex 1FQ9, red is FGF2-FGFR1-heparin ternary complex 8-2S-$^1C_4$ (red), green line is FGF2-FGFR1-heparin ternary complex 12-2S-$^1C_4$), **(b)** ligands in the FGF2-FGFR1-heparin ternary complex during a simulation time of 100 ns. (Black line is native heparin ligand 1FQ9, red line is heparin ligand 8-2S-$^1C_4$, and green data is heparin ligand 12-2S-$^1$C), **(c)** iduronic acid in the FGF2-FGFR1 ternary complex - heparin interaction during a simulation time of 100 ns. (Black data is native heparin IDS 1FQ9, red data is heparin IDS 8-2S-$^1C_4$, and green data is heparin IDS 12-2S-$^1C_4$)



The journal homepage www.jpacr.ub.ac.id
p-ISSN : 2302 – 4690 | e-ISSN : 2541 – 0733

The FGF2-FGFR1 ternary complex – native heparin 1FQ9 showed stability over 10 ns until the end of the simulation at around 0.69 nm. Meanwhile, the FGF2-FGFR1 ternary complex - heparin 8-2S-1C4 was stable at an RMSD value of around 0.97 nm after 25 ns of simulation. The initial fluctuations were smaller than those of the FGF2-FGFR1 ternary complex - heparin 12-2S-1C4, indicating higher initial stability. The higher initial stability of the FGF2-FGFR1 ternary complex - heparin 8-2S-1C4 is also reflected in the energy value of the docking results which is more negative than the FGF2-FGFR1 ternary complex-heparin 12-2S-1C4. Meanwhile, the FGF2-FGFR1 ternary complex - heparin 12-2S-1C4 experienced initial fluctuations of up to 45 ns, but finally stabilized at an RMSD value of around 0.89 nm until the end of the simulation. This indicates that the FGF2-FGFR1 ternary complex-heparin 12-2S-1C4 achieved higher stability at the end of the simulation than the FGF2-FGFR1 ternary complex-heparin 8-2S-1C4 [20]. In addition, the protein residue interaction at several time summarized in Table 5.

**Table 5.** Protein residue interaction at several simulation times

| Ligand | Simulation time (ns) | Amino acid residue interaction |
|---|---|---|
| Native | 25 | Ala 136, Arg 120, Arg 81, Asn 27, Gln 134, Lys 119, Lys 125, Lys 129, Lys 135, Lys 26, Lys 160, Lys 163, Lys 172, Lys 177, Lys 207, Arg 209, Thr 173 |
| 8-2S-$^1C_4$ | 8.8 | Arg 120, Arg 44, Lys 160, Lys 163, Asp 200, Glu 196, Lys 198, Lys 207 |
| 8-2S-$^1C_4$ | 20 | Arg 120, Lys 135, Glu 159, Lys 160 |
| 8-2S-$^1C_4$ | 100 | Arg 120, Asn 27, Lys 119, Lys 125, Lys 135 |
| 12-2S-$^1C_4$ | 0.9 | Arg 120, Arg 44, Lys 125, Lys 135, Lys 160, Arg 209, Lys 207, Val 208, Asp 200 |
| 12-2S-$^1C_4$ | 55 | Arg 120, Arg 44, Arg 209, Asp 200, Lys 207 |
| 12-2S-$^1C_4$ | 100 | Arg 120, Lys 119, Lys 125, Lys 129, Lys 135, Asp 200, Pro 199 |

**Analysis of amino acid residue root mean square fluctuation (RMSF)**

The amino acid residues in the FGF2-FGFR1 ternary complex -heparin 8-2S-1C4 that have high flexibility are Met 149, Asp 200, and Tyr 236 in the AC protein chain. Meanwhile, the in BD protein chain are Leu 269, Leu 359, and Met 149 (Figure 8). These residues are the residues with the largest position shifts during the simulation. However, all these residues are not key ligands in the binding of the FGF2-FGFR1 ternary complex to heparin.

It indicates that the function of heparin in binding FGFR1 and FGF2 can be said to be functioning well. There appeared to be quite high RMSF fluctuations in the region of amino acid residues 120 to around 209 in the AC chain which is the heparin binding site area, this indicates the less stable binding properties of 8-2S-1C4 heparin. Meanwhile, the BD chain did not show large fluctuations due to the binding of heparin 8-2S-1C4 after molecular dynamics only occurred in the BD chain, namely the FGF2 protein.



The journal homepage www.jpacr.ub.ac.id
p-ISSN : 2302 – 4690 | e-ISSN : 2541 – 0733

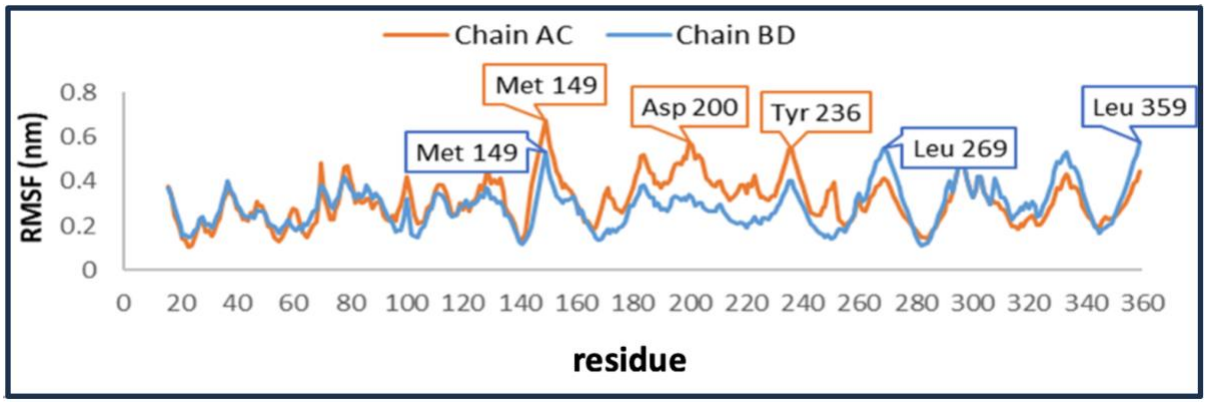


**Figure 8.** RMSF graph of amino acid residues of the FGF2-FGFR1 ternary complex - heparin 8-2S-$^{1}C_4$ in the AC chain (orange) and BD chain (blue).

Figure 9 shows the amino acid residues RMSF value in the FGF2-FGFR1 ternary complex - heparin 12-2S-1C4. The amino acid that have high flexibility are Gly 297, Pro 302, and Met 149 in both AC and BD protein chains. This residue is the residue with the largest position shift during the simulation. However, all these residues are not key ligands in the binding of FGFR1 and FGF2 to heparin. This shows that the function of heparin in binding FGFR1 and FGF2 can be said to be functioning well. There appears to be low RMSF fluctuation in the region of amino acid residues 120 to around 209 in both the AC and BD chains which are the heparin binding site areas, indicating that the binding properties of 12-2S-1C4 heparin in the FGF2-FGFR1 ternary complex are more stable. Residues Gly 297, Pro 302 which are at the end of the FGFR1 chain which bind directly to the transmembrane part of the receptor which shows high flexibility are thought to have an important role in tyrosine kinase activity and signal transduction in FGFR1 through allosteric changes in the receptor protein structure.

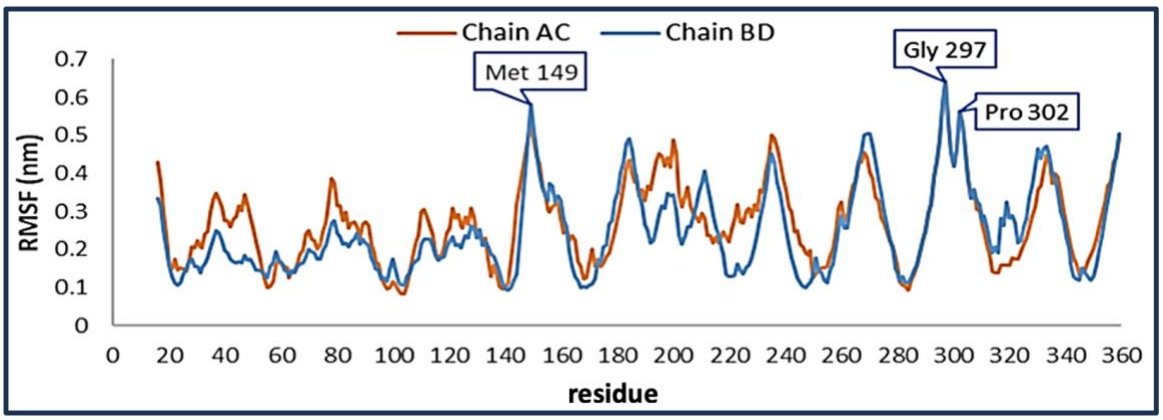


**Figure 9.** RMSF graph of amino acid residues of the FGFR1-FGF2 ternary complex - heparin 12-2S-$^{1}C_4$ in the AC chain (orange) and BD chain (blue).

Based on the research results, heparin 8-2S-1C4 binding energy to FGF2-FGFR1 ternary complex predicted by docking is -7.25 kcal/mol and there are many interactions at the active site, however after molecular dynamics simulations, interactions only occur with the ligand and FGF2 so it is less effective to stabilize the binding of FGF2-FGFR1 ternary complex as a



The journal homepage www.jpacr.ub.ac.id
p-ISSN : 2302 – 4690 | e-ISSN : 2541 – 0733

prerequisite for anticancer regulation signaling pathway ini FGFR1. Meanwhile, heparin 12-2S-1C4 has a binding energy predicted by docking of + 0.89 kcal/mol and has less interaction with the receptor ternary complex, but after molecular dynamics were carried out, the interaction between heparin and the FGF2-FGFR1 ternary complex was maintained until the end of the simulation. This is in accordance with research conducted by Cole, et al [13] who suggested that 2S heparin oligosaccharides from 2 saccharides to 12 saccharides cannot have an effect as anticancer compounds, because they have little effect on endothelial cell migration induced by FGF2 for angiogenic responses except 12 2S saccharides which provide an effect of 55% [13].

## CONCLUSION

This study demonstrates that heparin oligosaccharide length plays a critical role in stabilizing the FGF2-FGFR1 ternary complex. Although molecular docking predicted a more favorable initial binding for the 8-2S-1$C_4$ ligand, long-timescale molecular dynamics simulations revealed that the 12-2S-1$C_4$ ligand provides superior dynamic stability by maintaining simultaneous interactions with both FGF2 and FGFR1 throughout the simulation. The enhanced stability of the 12-saccharide complex offers a mechanistic explanation for its consistency with previously reported in vitro anti angiogenic and anticancer effects. These findings highlight the complementary value of molecular docking for assessing initial binding preferences and molecular dynamics simulations for capturing time-dependent stability, supporting the use of integrated in silico approaches to predict biologically relevant outcomes in heparin-mediated modulation of FGF2 signaling.

## REFERENCES

[1] World Cancer Research Fund. Worldwide cancer data. Available at: https://www.wcrf.org/preventing-cancer/cancer-statistics/worldwide-cancer-data/. Accessed 30 September 2025.
[2] Union for International Cancer Control. GLOBOCAN 2022: latest global cancer data shows rising incidence and stark inequalities. Available at: https://www.uicc.org/news-and-updates/news/globocan-2022-latest-global-cancer-data-shows-rising-incidence-and-stark. Accessed 30 September 2025.
[3] Zafar, A., Khatoon, S., Khan, M.J., Abu, J., and Naeem, A., *Discov. Onc.,* **2025**, 16 (1), 607.
[4] Colonna, G., *Cancers,* **2025**, 17 (13), 2102.
[5] Wang, P,. Chi, L., Zhang, Z., Zhao, H., Zhang, F., and Linhardt, R.J., *Carbohydr. Polym*., **2022**, 295, 119818.
[6] Koirala, N., Poudel, M., Shrivastava, A.K., Subba, R.K., Panthi, M., Paudel, S., Almarhoon, Z.M., Sharifi-Rad, J., and Calina, D., *Discov. Oncol.,* **2025**, 16(1), 231.
[7] Quan, Y., He, J., Zou, Q., Zhang, L., Sun, Q., Huang, H., Li, W., Xie, K., and Wei, F., *J. Immunotherap. Cancer.,* **2023**, 11 (8), e007080.
[8] Lee, J.H., Yang, S.B., Lee, J.H., Lim, H., Lee, S., Kang, T.B., Lim, J.H., Kim, Y.J., and Park, J., *Carbohydr. Polym.,* **2023**, 314, 120930.
[9] Giannas, E., and Kontovounisios, C., *J. Clin. Med*., **2023**, 12(22), 7173.
[10] Ornitz, D.M. and Itoh, N., *WIREs Mech. Dis.,* **2022**, 14(4), e1549.
[11] ten Dam, G.B., van de Wasterlo, E.M.A., Smetsers, T.F., Willemse, M., van Muijen, G.N., Merry, C.L., Gallagher, J.T., Kim, Y.S., and van Kuppevelt, T.H., *J. Biol. Chem*., **2004**, 279 (37), 38346-38352.



The journal homepage www.jpacr.ub.ac.id
p-ISSN : 2302 – 4690 | e-ISSN : 2541 – 0733

[12] Ling, L., Tan, S.K., Goh, T.H., Cheung, E., Nurcombe, V., van Vijnen, A.J., and Cool, S.M., *Mol Cancer.,* **2015***,* 14 (1), 136.
[13] Cole, C.L., Hansen, S.U., Baráth, M., Rushton, G., Gardiner, J.M., Avizienyte, E., and Jayson, G.C., *PLoS One.* **2010**, 5(7), 11644.
[14] Morris, G.M., Huey, R., Lindstrom, W., Sanner, M.F., Belew, R.K., Goodsell, D.S., and Olson, A.J., *J. Comput. Chem.,* **2009**, 30 (16), 2785-2791.
[15] BIOVIA, Dassault Systèmes. *Discovery Studio Visualizer*. San Diego: Dassault Systèmes, **2021**.
[16] Abraham, M.J., Murtola, T., Schulz, R., Páll, S., Smith, J.C., Hess, B., and Lindahl, E., *SoftwareX*, **2015**, 1-2, 19–25.
[17] Sari, I.W., Junaidin, J., and Pratiwi, D., *Jurnal Farmagazine*, **2020**, 7(2), 54-60.
[18] Ding, Y., Fang, Y., Moreno, J., Ramanujam, J., Jarrell, M., and Brylinski, M., *Comput. Biol. Chem*., **2016**, 64, 403-413.
[19] Zhou, H.X., and Pang, X., *Chem. Rev.,* **2018**, 118(4), 1691-1741.
[20] Salsabila, A.S., Safira, R.Z., Nugraha, A.R., Wulandari, D., Qaivani, R., and Sari, W.A., *Indonesian Journal of Biological Pharmacy*, **2023**, 3(3), 154-173.
[21] Soremekun, C., Jjingo, D., Kateete, D., Nash, O., Grallert, H., Peters, A., Chikowore, T., Batini, C., Soremekun, O., and Fatumo, S., *Next Res.*, **2024**, 1(2), 100041.



**The journal homepage www.jpacr.ub.ac.id**
**p-ISSN : 2302 – 4690 | e-ISSN : 2541 – 0733**